厚生労働科学研究費補助金（第３次対がん総合戦略研究事業）
分担研究報告書

低レベルPhIPの持続的曝露により誘発されるDDRの分子機構の解明

分担研究者　　山下克美
金沢大学医薬保健研究域　准教授

研究要旨　本研究では、DDR の初期過程としての細胞周期停止に焦点を当て、ゲノム損傷初期に分解が誘発される Cdc25A と後期に分解が誘発される Cdc25B について、DDR 誘発性分解に関わる遺伝子を解明する。本年度は、遺伝子の分離のためのスクリーニング系の構築を行った。ゲノム損傷誘発性分解に関わる Cdc25A と Cdc25B の N-末端領域をコードする cDNA 断片をそれぞれ EGFP または RFP と融合させたプローブ遺伝子を構築し、HeLa 細胞にて安定発現株を分離した。分離された細胞に DNA 損傷や DNA 複製阻害等の刺激を与えたところ、Cdc25A/N-EGFP は約 1 時間で、Cdc25B/N-RFP は約 8 時間で蛍光が消失し、またタンパク質の分解も確認された。以上より、Cdc25A/B の DDR 誘発性分解制御に関わる遺伝子スクリーニングに使用可能な細胞が分離されたと考えられた。

A．研究目的

本研究では、疾患モデル動物を用いた環境発がん機構解明のうち、代表的な環境発がん物質である PhIP による発がんの初期過程を明らかにする。特に、本研究では動物レベルでは解明が困難な、発がんの初期過程である DDR のうち、細胞周期停止機構の解明を目指す。そのために、ゲノム損傷を受けた細胞で、1 時間以内に分解が誘発される Cdc25A の安定性制御に関わる新規遺伝子の分離を目指す。また、対照として、遅れて分解が誘発される Cdc25B の安定性制御に関わる遺伝子についても解析する。

B．研究方法

Cdc25A や Cdc25B の分解誘発系を解明するために、siRNA や shDNA ライブラリーを細胞へ導入し、ゲノム損傷刺激に対しても Cdc25A や Cdc25B の分解が誘発されない siRNA や shDNA を分離する。この目的のために今年度は、遺伝子を分離するためにライブラリーを導入する細胞の構築を行った。

即ち、Cdc25A/Cdc25B におけるゲノム損傷ストレス応答性分解の制御領域である N-末端断片をそれぞれ EGFP または RFP と融合させたプローブ遺伝子を構築した。これらを HeLa 細胞へ導入し蛍光タンパク質を発現する細胞株を分離した。

これらの細胞にたいし、ゲノム損傷薬剤としてエトポシドを 10 mM で、DNA 合成阻害剤としてヒドロキシウレアを 10 mM で処理し、時間を追って蛍光と各タンパク質の発現を検討した。

（倫理面への配慮）

培養細胞使用実験のため、特になし。

C．研究結果

本年度は、モデルシステムとして HeLa 細胞を用いた遺伝子同定システムの検討を行った。まず、Cdc25A および Cdc25B のストレス誘発性分解制御に係る N-末端側 150－170 アミノ酸をコードする cDNA をそれぞれ GFP または RFP と融合させ、Cdc25A/N-EGFP と Cdc25B/N-RFP を構築した。

これらの「分解検出用プローブ遺伝子」を HeLa 細胞へ導入し、安定発現細胞株を分離した。さらに、それぞれの遺伝子を単独で発現する HeLa 細胞株も分離した。

これらを用いて、遺伝毒性ストレス即ちエトポシドによる DNA 損傷誘発と、非遺伝毒性ストレス即ち NaCl 処理を行い、蛍光の消失を検討した。その結果、Cdc25A/N の緑色蛍光は両薬剤処理 1 時間

以内に消失したが、Cdc25B/N 由来の赤色蛍光は NaCl 処理の場合は 1 時間以内に消失し、エトポシド処理の場合は約 8 時間後に完全な消失が観察された。

D．考察

今年度の研究により、DDR 応答として Cdc25A や Cdc25B の分解を誘発するシグナル伝達に係る遺伝子を分離するシステムの原理が完成したと考えられるため、来年度以降はこのシステムを用いて遺伝子の探索が可能となった。

Cdc25A は DDR として、ゲノム損傷誘発後 30 分以内に分解が誘発される。これは、Cdc25A 分子内に恒常的分解に係る部位と、損傷誘発性分解に係る部位が存在し、細胞内のタンパク量が低く抑えられているためである。本研究に用いたプローブでは N-末端側の「DDR としての分解に係る部位」のみを用いているために、分解のキネティクスが遅いようであるが、これは上述の理由によるものと思われる。

以上、今年度の研究により、DDR 応答として Cdc25A や Cdc25B 分解をもたらす遺伝子群の同定が可能となった。

E．結論

本研究では、DDR 初期応答として細胞制御因子の分解誘発を制御する遺伝子を、siRNA や shDNA ライブラリーを細胞へ導入することにより同定する。

そのための指標として、ゲノム損傷により分解が速やかに誘導される Cdc25A と、遅れて分解が誘発される Cdc25B を選択した。それぞれの遺伝子において外因性ストレス誘発性分解制御に係る N-末端領域を蛍光タンパク質と融合し、Cdc25A/N-EGFP と Cdc25B/N-RFP を作成したのち、各プローブ遺伝子を HeLa 細胞へ導入し、安定発現細胞を樹立した。

これらの細胞中で発現する蛍光タンパク質は、細胞へのストレス刺激に応じて分解が誘発されたことから、このような細胞株を目的の遺伝子スクリーニングに用いることは可能と思われる。

F．研究発表

1. 論文発表

1. Yamashita Y, Kasugai I, Sato, M Tanuma N, Yamashita K, Nomura M, Sonoda Y, Kumabe T, Tominaga T, Katakura R, and Shima H.: CDC25A mRNA levels significantly correlate with Ki-67 expression in human glioma samples. J. Neuro-oncol., 100: 43-49 (2010).
2. Uchida S, Watanabe N, Kudo Y, Yoshioka K, Matsunaga T, Ishizaka Y, Nakagama H, Poon RYC, and Yamashita K.: SCF^{bTrCP} mediates stress-activated MAP kinases-induced Cdc25B degradation. J. Cell Sci., in press

2. 学会発表

1. 山下克美、内田早苗、中釜斉：環境発がん物質による細胞周期制御因子 Cdc25 の分解機構．第 39 回日本環境変異原学会大会（2010 年 11 月、つくば市）
2. 内田早苗、渡辺信元、工藤保誠、松永司、中　釜斉、山下克美．SCF^{bTrCP} による Cdc26B 分解における PEST 配列の役割．第 33 回日本分子生物学会年会・第 83 回日本生化学会大会合同大会（2010 年 12 月、神戸）

G．知的所有権の取得状況

1. 特許取得

なし。

2. 実用新案登録

なし。

3. その他

特記すべきものなし。

研究成果の刊行に関する一覧表

書籍

著者氏名	論文タイトル名	書籍全体の編集者名	書籍名	出版社名	出版地	出版年	ページ
Masutani M., Shirai H., Ogino H., Poetsch A., Sasamoto E., Maeda D., Hashimoto A., Sugimura T.	Role of poly-ADP-ribosylation in the maintenance of genomic stability.	Nishimura S., Loeb L.A., Masutani M., Nakagama H., Sekiya T.	Extended Abstracts for The 40th International Symposium of the Princess Takamatsu Cancer Research Fund: DNA Repair and Human Cancers	Princess Takamatsu Cancer Research Fund	Tokyo	2010	76-79
中島 淳, 平石秀幸	メタボ(内臓肥満)と消化器の病気	坪内博仁	消化器 now	日本消化器病学会	東京	2010	2-3
高橋宏和, 内山崇, 中島 淳	内臓脂肪およびアディポネクチンと大腸発癌の性差	内田章義	消化器内科	科学評論社	東京	2010	315-319
高橋宏和, 細野邦広, 中島 淳	Aberrant crypt foci とサプリメントの相関解析	三浦総一郎	消化と吸収	日本消化吸収学会	東京	2010	43-46
高橋宏和, 遠藤宏樹, 中島 淳	肥満と大腸癌	坪内博仁	肥満と消化器疾患	日本消化器病学会	東京	2010	119-133
T. Tsuzuki, T. Isoda, J. Piao, K. Sakumi, Y. Nakabeppu, Y. Nakatsu。	Oxidative stress-induced tumorigenesis in the small intestines of DNA repair-deficient mice	Eds. S. Nishimura, L. A. Loeb, M. Masutani, H. Nakagama, T. Sekiya	International Proceedings: The 40th International Symposium of the Princess Takamatsu Cancer Research Fund	Princess Takamatsu Cancer Research Fund	Tokyo	2010	28-34

雑誌

発表者氏名	論文タイトル名	発表誌名	巻号	ページ	出版年
Wang R, Dashwood W-M, Nian H, Löhr CV, Fischer KA, Tsuchiya N, Nakagama H, Ashktorab H, Dashwood RH	NADPH oxidase overexpression in human colon cancers and rat colon tumors induced by 2-amino-1-methyl-6-phenylimidazo[4,5-b]pyridine (PhIP)	Int. J. Cancer	128	2581-2590	2010
Izumiya M, Okamoto K, Tsuchiya N, Nakagama H	Functional screening using a microRNA virus library and microarrays: a new high-throughput assay to identify tumor-suppressive microRNAs	Carcinogenesis	31	1354-1359	2010
Tsuchiya N, Nakagama H	MicroRNA, SND1, and alterations in translational regulation in colon carcinogenesis	Mutation Research	693	94-100	2010
中釜 斉	マイクロRNAと癌	細胞	42	2(226)-3(227)	2010
泉谷昌志、土屋直人、中釜 斉	機能スクリーニング系によるがん抑制的miRNAの単離	生体の科学	61	4(315-320)	2010
筆宝義隆、中釜 斉	メタボリックシンドローム-基礎・臨床の最新知見-	日本臨牀	69	438-443	2010
泉谷昌志、中釜 斉	大腸癌-最新の研究動向-癌遺伝子と癌抑制遺伝子	日本臨牀	69	3:72-76	2010
Osada T, Ogino H, Hino T, Ichinose S, Nakamura K, Omori A, Noce T, Masutani M.	PolyADP-ribosylation is required for pronuclear fusion during postfertilization in mice.	PLoS ONE	5	e12526	2010
Shirai H, Hirai T, Sasamoto E, Inase A, Ogino H, Sasai K, Sugimura T, Masutani M.	Role of Poly(ADP-ribosylation) Reaction in Response to Ionizing Radiation.	Radiological Sciences	53	69-71	2010
Kosaka N, Iguchi H, Yoshioka Y, Takeshita F, Matsuki Y, Ochiya T.	Secretory mechanisms and intercellular transfer of microRNAs in living cells.	J. Biol. Chem.	285	17442-17452	2010
Satow R, Shitashige M, Kanai Y, Takeshita F, Ojima H, Jigami T, Honda K, Kosuge T, Ochiya	Combined Functional Genome Survey of Therapeutic Targets for Hepatocellular Carcinoma.	Clin. Cancer Res.	16	2518-2528	2010

T, Hirohashi S, Yamada T.					
Kawamata M, Ochiya, T.	Generation of genetically modified rats from embryonic stem cells.	Proc Natl Acad Sci USA.	107	14223-14228	2010
Ikawa, T, Hirose S, Masuda K, Kakugawa K, Satoh R, Shibano-Satoh A, Kominami R, Katsura Y, Kawamoto H.	An essential developmental checkpoint for production of the T cell lineage.	Science	329	93-96	2010
Go R, Hirose S, Morita S, Yamamoto T, Katsuragi Y, Mishima Y, Kominami R.	Bcl11b heterozygosity promotes clonal expansion and differentiation arrest of thymocytes in γ-irradiated mice.	Cancer Science	101	1347-1353	2010
Yamamoto T, Morita S, Go E, Obata M, Katsuragi Y, Fujita Y, Maeda Y, Yokoyama M, Aoyagi Y, Ichikawa H, Mishima Y, Kominami R.	Clonally expanding thymocytes having lineage capability in γ-ray induced mouse atrophic thymus.	Int. J. Radiation Oncology Biol Phys	77	235-243	2010
Okumura H, Miyasaka Y, Morita Y, Nomura T, Mishima Y, Takahashi S, Kominami R.	Bcl11b Heterozygosity Leads to Age-Related Hearing Loss and Degeneration of Outer Hair Cells of the Mouse Cochlea.	Experimental Animals		in press.	2011
Hosono K, Endo H, Takahashi H, Sugiyama M, Uchiyama T, Suzuki K, Nozaki Y, Yoneda K, Fujita K, Yoneda M, Inamori M, Tomatsu A, Chihara T, Shimpo K, Nakagama H, Nakajima A	Metformin suppresses azoxymethane-induced colorectal aberrant crypt foci by activating AMP-activated protein kinase.	Carcinogenesis	49	662-671	2010
Nakajima A, Endo H, Yoneda K, Fujisawa T, Sugiyama M, Hosono K, Nozaki Y, Takahashi H, Fujita K, Yoneda M, Inamori M, Shimamura T,	Molecular mechanisms linking adiponectin receptor signalling and cancer.	he Open Obesity Journal	2	43-49	2010

Kobayashi N, Kirikoshi H, Kubota K, Saito S, Wada K, Nakagama H					
Hosono K, Endo H, Takahashi H, Sugiyama M, Sakai E, Uchiyama T, Suzuki K, Iida H, Sakamoto Y, Yoneda K, Koide T, Tokoro C, Abe Y, Inamori M, Nakagama H, Nakajima A	Metformin suppresses colorectal aberrant crypt foci in a short-term clinical trial.	Cancer Prev Res	3	1077-1083	2010
Takahashi H, Hosono K, Uchiyama T, Sugiyama M, Sakai E, Endo H, Maeda S, Schaefer KL, Nakagama H, Nakajima A	PPARgamma ligand as a promising candidate for colorectal cancer chemoprevention: A pilot study.	PPAR Res	2010	257835	2010
Uchiyama T, Takahashi H, Sugiyama M, Sakai E, Endo H, Hosono K, Yoneda K, Yoneda M, Inamori M, Nagashima Y, Inayama Y, Wada K, Nakajima A	Leptin receptor is involved in STAT3 activation in human colorectal adenoma.	Cancer Sci.	102	367-372	2010
内山崇，高橋宏和，中島　淳	メタボリックシンドロームと大腸癌	G. I. Research	18	23-28	2010
高橋宏和，内山崇，中島淳	内臓脂肪およびアディポネクチンと大腸発癌の性差	消化器内科	50	315-319	2010
高橋宏和，細野邦広，中島淳	大腸発がんにおけるレジスチンおよびTNF-αの相関解析	消化と吸収	33	262-264	2010
高橋宏和，遠藤宏樹，中島淳	肥満と大腸癌	肥満と消化器疾患		119-133	2010
Oshima H, Oshima M.	Mouse models of gastric tumors: Wnt activation and PGE_2 induction.	Pathol Int	60	599-607	2010
Oshima H, Hioki K, Popivanova BK, Oguma K, van Rooijen N, Ishikawa TO, Oshima M.	Prostaglandin E_2 signaling and bacterial infection recruit tumor-promoting macrophages to mouse gastric tumors.	Gastroenterology	140	596-607	2011
Oshima H,	Activation of epidermal growth	Cancer Sci	102	713-71	2011

Popivanova BK, Oguma K, Kong D, Ishikawa TO, Oshima M.	factor receptor signaling by the prostaglandin E_2 receptor EP4 pathway during gastric tumorigenesis.			9	
Deguchi A, Miyoshi H, Kojima, Y, Okawa K, Aoki M, Taketo MM.	LKB1 suppresses p21-activated kinase-1 (PAK1) by phosphorylation of Thr109 in the p21-binding domain.	J Biol. Chem.	285	18282-18290	2010
Kitamura T, Fujishita T, Loetscher P, Revesz L, Hashida H, Kizaka-Kndoh S, Aoki M, Taketo MM.	Inactivation of chemokine (C-C motif) receptor 1 (CCR1) suppresses colon cancer liver metastasis by blocking accumulation of immature myeloid cells in a mouse model.	Proc. Natl. Acad. Sci. USA	107	13063-13068	2010
Sonoshita M, Aok, M, Fuwa H, Aoki K, Hosogi H, Sakai Y, Hashida H, Takabayashi A, Sasaki M, Robine S, Itoh K, Yoshioka K, Kakizaki F, Kitamura T, Oshima M, Taketo MM.	Suppression of colon cancer metastasis by Aes through inhibition of Notch signaling.	Cancer Cell	19	125-137	2011
Aoki K, Kakizaki F, Sakashita H, Manabe T, Aoki M, Taketo MM.	Suppression of colonic polyposis by homeoprotein CDX2 through its non-transcriptional function that stabilizes $p27^{Kip1}$.	Cancer Res.	71	593-602	2011
Kuramoto T, Yokoe M, Yagasaki K, Kawaguchi T, Kumafuji K, Serikawa T.	Genetic analyses of fancy rat-derived mutations.	Exp Anim.	59	147-155	2010
Kuramoto T, Kuwamura M, Tagami F, Mashimo T, Nose M, Serikawa T.	Kyoto rhino rats derived by ENU mutagenesis undergo congenital hair loss and exhibit focal glomerulosclerosis.	Exp Anim.	60	57-63	2011
Kuramoto T, Kuwamura M, Tokuda S, Izawa T, Nakane Y, Kitada K, Akao M, Guénet JL, Serikawa T.	A mutation in the gene encoding mitochondrial Mg2+ channel MRS2 results in demyelination in the rat.	PLoS Genet.	7	e1001262	2011
Tsuzuki T, Piao J, Isoda T, Sakumi K,	Oxidative stress-induced tumorigenesis in the small intestine	Health Physics	100	293-294	2011

Nakabeppu Y, Nakatsu Y.	of various types of DNA repair-deficient mice				
N. Sagata, A. Iwaki, T. Aramaki, K. Takao, S. Kura, T. Tsuzuki, R. Kawakami, I. Ito, T. Kitamura, H. Sugiyama, T. Miyakawa, and Y. Fukumaki	Comprehensive behavioral study of GluR4 knockout mice: implication in cognitive function.	Genes, Brain Behavior	9	899-909	2010
Nakamura T, Meshitsuka S, Kitagawa S, Abe N, Yamada J, Ishino T, Nakano H, Tsuzuki T, Doi T, Kobayashi Y, Fujii S, Sekiguchi M, Yamagata Y.	Structural and dynamic features of the MutT protein in the recognition of nucleotides with the mutagenic 8-oxoguanine base.	J. Biol. Chem.	285	444-452	2010
Yamashita Y, Kasugai I, Sato M, Tanuma N, Yamashita K, Nomura M, Sonoda Y, Kumabe T, Tominaga T, Katakura R, Shima H.	CDC25A mRNA levels significantly correlate with Ki-67 expression in human glioma samples.	Journal of Neuro-oncology	100	43-49	2010

ROLE OF POLY-ADP-RIBOSYLATION IN THE MAINTENANCE OF GENOMIC STABILITY

Mitsuko Masutani, Hidenori Shirai, Hideki Ogino, Anna Poetsch, Erika Sasamoto, Daisuke Maeda, Aki Hashimoto and Takashi Sugimura

Biochemistry Division

National Cancer Center Research Institute

1-1, Tsukiji, 5-chome, Chuo-ku, Tokyo 104-0045, Japan

(mmasutan@ncc.go.jp)

Poly-ADP-ribosylation is a unique post-translational modification catalyzed by poly(ADP-ribose) polymerase (PARP) using β-NAD^+ as a substrate. PARP-1 is activated by DNA strand breaks and is involved in DNA repair pathways, including base excision repair (BER) and single and double strand break repairs. PARP-1 is also involved in the regulation of transcription and chromatin function. Poly(ADP-ribose) is degraded mainly by poly(ADP-ribose) glycohydrolase (PARG) to ADP-ribose in the cells.

We have investigated the role of PARP-1 and PARG in the maintenance of genomic stability and carcinogenesis. *Parp-1*$^{-/-}$ mice[1] showed increased incidence of tumors induced by alkylating agents, including *N*-nitrosobis (2-hydroxypropyl) amine (BHP)[2]. No increase in the incidence was observed in the case with 4-nitroquinoline 1-oxide (4NQO)[3]. This susceptibility difference may reflect the active involvement of PARP-1 in BER and strand break repair working after alkylation damage on DNA but not nucleotide excision repair, which targets bulky DNA adducts induced by 4NQO.

The frequencies of both simple and complex-type deletion mutations, but not base substitution mutations, were augmented in the livers of *Parp-1*$^{-/-}$ compared to *Parp-1*$^{+/+}$ mice after BHP treatment[4]. *Parp-1* deficiency also caused an increase of deletion mutations in the liver at an advanced age[5]. PARP-1 is thus involved in suppressing imprecise repair of DNA damage leading to deletion mutation. This role of PARP-1 was further confirmed by a cell-free repair assay system of double strand breaks.

On the other hand, when we analyzed mutations in *Parp-1*$^{+/+}$ and *Parp-1*$^{-/-}$ mice 3 days after γ-irradiation at 8 Gy, the frequencies of deletion mutation were increased 3-fold in *Parp-1*$^{+/+}$ mice by γ-irradiation, whereas the those in *Parp-1*$^{-/-}$ mice were not increased as in

the case of knockout mice defective in end-joining repair.

Specific and potent PARP inhibitors have been developed and are now in clinical trials of cancers. Because *Parp-1*$^{-/-}$ mice showed increased susceptibility to tumor induction by alkylating agents[2,6] and higher frequencies of deletion mutations and other genomic instabilities[3,7], there is a possibility that the long-term effect of PARP inhibitors on genomic instability and cancer risk could be a potential problem in therapeutic use.

Parg$^{-/-}$ mouse ES cell lines, established by disrupting both alleles of *Parg* exon 1, exhibited enhanced lethality after γ-irradiation, treatment with cisplatin[8] and methylmethanesulfonate (MMS) compared with wild-type ES cells. After MMS treatment, early events were enhanced, such as accumulation of poly(ADP-ribose), p53 network activation, NAD depletion, γH2AX foci formation and S-phase arrest in *Parg*$^{-/-}$ ES cells. Later, the cell death processes, including caspase activation, and DNA fragmentation, were augmented. These results suggest the possibility that PARG is also involved in DNA damage response and functional inhibition of PARG possibly leads to sensitization of tumor cells to chemo- and radiation therapies. There are only a few PARG inhibitors available and the development of new specific PARG inhibitors is expected.

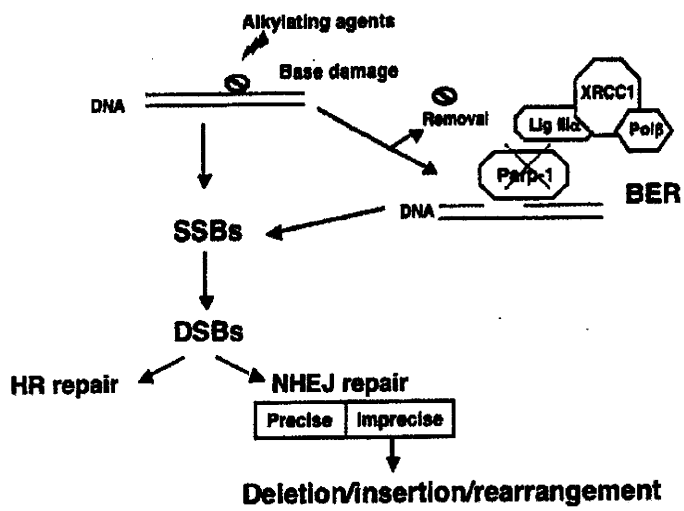

Figure 1 Model for DNA repair response under *Parp-1* deficiency.

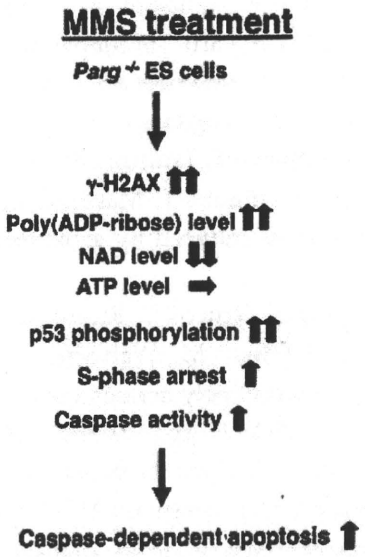

Figure 2 Enhanced lethality after MMS treatment in *Parg*$^{-/-}$ ES cells.

References

1. Masutani M, Suzuki H, Kamada N, Watanabe M, Ueda O, Nozaki T, Jishage K, Watanabe T, Sugimoto T, Nakagama H, Ochiya T, Sugimura T. Poly(ADP-ribose) polymerase gene disruption conferred mice resistant to streptozotocin-induced diabetes. Proc. Natl. Acad. Sci. USA, 96: pp.2301-2304, 1999
2. Tsutsumi M, Masutani M, Nozaki T, Kusuoka O, Tsujiuchi T, Nakagama H, Suzuki H, Konishi Y, Sugimura T. Increased susceptibility of poly(ADP-ribose) polymerase-1 knockout mice to nitrosamine carcinogenicity. Carcinogenesis, 22: pp.1-3, 2001
3. Gunji A, Uemura A, Tsutsumi M, Nozaki T, Kusuoka O, Omura K, Suzuki H, Nakagama H, Sugimura T, Masutani M. *Parp-1* deficiency does not increase the frequency of tumors in the oral cavity and esophagus of ICR/129Sv mice by 4-nitroquinoline 1-oxide, a carcinogen producing bulky adducts. Cancer Lett., 241:pp.87-92, 2006
4. Shibata A, Kamada N, Masumura K, Nohmi T, Kobayashi S, Teraoka H, Nakagama H, Sugimura T, Suzuki H, Masutani M. *Parp-1* deficiency causes an increase of deletion mutations and insertions/rearrangements *in vivo* after treatment with an alkylating agent. Oncogene, 24: pp.1328-1337, 2005

5. Shibata A, Maeda D, Ogino H, Tsutsumi M, Nohmi T, Nakagama H, Sugimura T, Teraoka H, Masutani M. Role of Parp-1 in suppressing spontaneous deletion mutation in the liver and brain of mice at adolescence and advanced age. Mutat. Res./Fundamental and Molecular Mechanisms of Mutagenesis, 664: pp.20-27, 2009
6. Nozaki T, Fujihara H, Watanabe M, Tsutsumi M, Nakamoto K, Kusuoka, O, Kamada N, Suzuki H, Nakagama H, Sugimura T, Masutani M. *Parp-1* deficiency implicated in colon and liver tumorigenesis induced by azoxymethane. Cancer Sci., 94:pp.497-500, 2003
7. de Murcia JM, Niedergang C, Trucco C, Ricoul M, Dutrillaux B, Mark M, Oliver FJ, Masson M, Dierich A, LeMeur M, Walztinger, C, Chambon, P, de Murcia, G. Requirement of poly(ADP-ribose) polymerase in recovery from DNA damage in mice and in cells. Proc Natl Acad Sci USA, 94: pp.7303-7307, 1997
8. Fujihara H, Ogino H, Maeda D, Shirai H, Nozaki T, Kamada N, Jishage K, Tanuma S, Takato T, Ochiya T, Sugimura T, Masutani M. Poly(ADP-ribose) glycohydrolase deficiency sensitizes mouse ES cells to DNA damaging agents. Current Cancer Drug Targets, In press.

Dr. Mitsuko Masutani, Ph.D.

1985	MS, Okayama University
1988	Ph.D., University of Tokyo
1988-1989	Research Fellow, JSPS, University of Tokyo
1989-1992	Research Resident Fellow, National Cancer Center Research Institute (NCCRI)
1992-1997	Research Staff, Biochemistry Division, NCCRI
1997-2007	Section Head, Biochemistry Division, NCCRI
2005-2008	Project Leader, ADP-ribosylation in Oncology Project NCCRI
2007-	Chief, Biochemistry Division, NCCRI

Specialty and Present Interest:
Poly-ADP-ribosylation, Biochemistry, Carcinogenesis, Cancer Prevention and Treatment

UICC
global cancer control

IJC
International Journal of Cancer

NADPH oxidase overexpression in human colon cancers and rat colon tumors induced by 2-amino-1-methyl-6-phenylimidazo[4,5-*b*]pyridine (PhIP)

Rong Wang[1], Wan-Mohaiza Dashwood[1], Hui Nian[1,2], Christiane V. Löhr[3], Kay A. Fischer[3], Naoto Tsuchiya[4], Hitoshi Nakagama[4], Hassan Ashktorab[5] and Roderick H. Dashwood[1,6]

[1] Linus Pauling Institute, Oregon State University, Corvallis, Oregon
[2] Department of Biochemistry and Biophysics, Oregon State University, Corvallis, Oregon
[3] College of Veterinary Medicine, Oregon State University, Corvallis, Oregon
[4] Biochemistry Division, National Cancer Center Research Institute, Tokyo, Japan
[5] Howard University College of Medicine, Washington, DC
[6] Department of Environmental and Molecular Toxicology, Oregon State University, Corvallis, Oregon

NADPH oxidase/dual-oxidase (Nox/Duox) family members have been implicated in nuclear factor kappa-B (NFκB)-mediated inflammation and inflammation-associated pathologies. We sought to examine, for the first time, the role of Nox/Duox and NFκB in rats treated with the cooked meat heterocyclic amine carcinogen 2-amino-1-methyl-6-phenylimidazo[4,5-*b*]pyridine (PhIP). In the PhIP-induced colon tumors obtained after 1 year, Nox1, Nox4, NFκB-p50 and NFκB-p65 were all highly overexpressed compared with their levels in adjacent normal-looking colonic mucosa. Nox1 and Nox4 mRNA and protein levels also were markedly elevated in a panel of primary human colon cancers, compared with their matched controls. In HT29 human colon cancer cells, Nox1 knockdown induced G1 cell cycle arrest, whereas in Caco-2 cells there was a strong apoptotic response, with increased levels of cleaved caspase-3, -6, -7 and poly(ADP-ribose)polymerase. Nox1 knockdown blocked lipopolysaccharide-induced phosphorylation of IκB kinase, inhibited the nuclear translocation of NFκB (p50 and p65) proteins, and attenuated NFκB DNA binding activity. There was a corresponding reduction in the expression of downstream NFκB targets, such as *MYC*, *CCND1* and *IL1β*. The results provide the first evidence for a role of Nox1, Nox4 and NFκB in PhIP-induced colon carcinogenesis, including during the early stages before tumor onset. Collectively, the findings from this investigation and others suggest that further work is warranted on the role of Nox/Duox family members and NFκB in colon cancer development.

Key words: colon carcinogenesis, heterocyclic amines, NFκB, reactive oxygen species, apoptosis

Abbreviations: GAPDH: glyceraldehyde-3-phosphate dehydrogenase; IKK: IκB kinase; IL-1β: interleukin-1β; IL6: interleukin-6; NFκB: nuclear factor kappa-B; Nox/Duox: NAPDH oxidase/dual-oxidases; LPS: lipopolysaccharide; MTT: 3-(4,5-dimethythiazol-2-yl)-2,5-diphenyltetrazolium bromide; PARP: poly(ADP-ribose)polymerase; PhIP: 2-amino-1-methyl-6-phenylimidazo[4,5-*b*]pyridine; TMAs: tissue microarrays; TNF-α: tumor necrosis factor-α; TNFR: TNF receptor

Additional supporting information may be found in the online version of this article.

Grant sponsor: National Cancer Institute; **Grant numbers:** CA90890, CA65525, CA90176, CA122959; **Grant sponsor:** National Institute of Environmental Health Sciences; **Grant number:** P30 ES00210; **Grant sponsor:** Foundation for Promotion of Cancer Research

DOI: 10.1002/ijc.25610

History: Received 22 Mar 2010; Accepted 27 Jul 2010; Online 16 Aug 2010

Correspondence to: Roderick H. Dashwood, Linus Pauling Institute, Oregon State University, Corvallis, OR 97331, USA, Tel.: +1-541-737-5086, Fax: +1-541-737-5077, E-mail: Rod.Dashwood@oregonstate.edu

Nuclear factor kappa-B (NFκB) is a key transcription factor regulating the expression of genes involved in inflammation, immune modulation and apoptosis, as well as in various stages of cancer development.[1–3] In mammals, five members of the NFκB family have been identified, p50, p65 (RelA), RelB, c-Rel and p52.[4] These subunits exist as homodimers or heterodimers, under the control of inhibitors of NFκB (IκB). The IκB family comprises IκBα, IκBβ, IκBγ, IκBε, IκBζ, BCL3, p100 and p105. Activation of NFκB involves IκB kinase (IKK)-dependent phosphorylation and degradation of IκB proteins.[5] IKK contains the catalytic subunits IKKα and IKKβ, and a regulatory component, IKKγ/NEMO. Nuclear trafficking of NFκB results in the activation of genes encoding cytokines, chemokines, growth factors and antiapoptotic factors.[1]

A plethora of physiological stimuli activate NFκB. These include lipopolysaccharide (LPS) and proinflammatory cytokines, such as interleukin-6 (IL6) and interleukin-1β (IL-1β), as well as tumor necrosis factor-α (TNF-α), acting *via* the TNF receptor (TNFR). Activation of NFκB is associated with the production of reactive oxygen species (ROS), and the best-studied ROS-producing enzyme is the phagocyte-derived NADPH oxidase (Nox), which plays a pivotal role during

bacterial infection and inflammation.[6,7] Non–phagocyte-derived Nox homologues also have been identified, designated collectively as the Nox/dual oxidase (Duox) family, which comprises Nox1, Nox2, Nox3, Nox4 and Nox5, plus Duox1 and Duox2.[8] Each Nox/Duox isoform exhibits a distinct cellular and tissue distribution pattern.[7] In lung, aberrant expression of Nox2, Duox1 and Duox2 contributes to chronic obstructive pulmonary disease, asthma and cystic fibrosis,[9] whereas in forebrain abnormal levels of Nox2 and Nox4 have been implicated in the pathogenesis of schizophrenia.[10]

Accumulating evidence supports a role for Nox/Duox members in other pathologies, including cancer. Nox1 stimulates mitogenesis, cell transformation and tumorigenesis when ectopically expressed in NIH3T3 fibroblasts and DU-145 prostate epithelial cells, with a corresponding increase in angiogenesis.[11,12] Overexpression of Nox1 was observed in prostate, breast and ovarian cancers,[13,14] and Nox4 was detected at high levels in glioblastoma cells.[15] Information on Nox/Duox involvement in colon cancer is somewhat inconsistent. Geiszt *et al.*[16] first reported that Nox 1 was expressed mainly in differentiated colonic epithelial cells, and Szanto *et al.*[17] detected no statistical difference for *NOX1* mRNA expression between adenomas and poorly- or well-differentiated colon adenocarcinomas. Szanto *et al.*[17] concluded that Nox1 is an enzyme that is constitutively expressed in colonic epithelium and is not associated with tumorigenesis. However, using immunohistochemical analyses, Fukuyama *et al.*[18] observed Nox1 overexpression in human colon adenomas and well-differentiated adenocarcinomas, and Laurent *et al.*[19] reported that Nox1 was overexpressed in human colon cancers and was correlated with activating mutations in K-ras.

To clarify the role of Nox/Duox family members during colon carcinogenesis, rats were treated with the heterocyclic amine 2-amino-1-methyl-6-phenylimidazo[4,5-*b*]pyridine (PhIP), as reported before,[20,21] and the expression levels of Nox/Duox and NFκB were examined before and after the appearance of frank tumors. A panel of primary human colon cancers and human colon cancer cell lines also was studied for expression of NFκB and Nox/Duox isoforms.

Material and Methods

Rat colon tumors

Colon tumors and adjacent normal-looking mucosa were from a study in which male F344 rats received intermittent exposure to PhIP alternating with a high-fat diet, as reported elsewhere.[20] An interim sacrifice was included to assess early molecular changes, before the onset of tumors. Specifically, 24 h after the last dose of PhIP, rats in each group ($n = 5$) were euthanized, the colon was removed and opened longitudinally, and the mucosa was scraped and frozen in liquid nitrogen before storing at −80°C. The remaining animals in each group ($n = 36$) were euthanized at 52 weeks (Supporting Information Fig. 1). A complete necropsy examination was performed on each animal.[20] This work received prior approval from the Institutional Animal Care and Use Committee.

Human primary colon cancers

Ten pairs of primary human colon cancers and their matched adjacent normal-looking tissues were kindly provided by Steven F. Moss, M.D. and Lelia Simao (Rhode Island Hospital, Providence, RI). The patients (6 female, 4 male, 53-93 years of age) had been diagnosed with adenocarcinoma of the colon.

Quantitative real-time RT-PCR (qPCR)

Frozen colon tumor samples and their matched controls were thawed, and mRNA was extracted using the RNeasy kit (Qiagen, Valencia, CA). RNA (2 μg) was reverse-transcribed in 20 μl of 1X RT buffer, containing 10 U RNase inhibitor (Invitrogen, Carlsbad, CA), 0.5 mM each dNTP, 4 U Omniscript Reverse Transcriptase (Qiagen) and 50 ng random hexamers (Invitrogen). Primers were as listed in Supporting Information Table I. Forty cycles of PCR were run on an Opticon Monitor 2 system (Finnzymes, Finland), in 20 μl total reaction volume containing cDNAs, SYBR Green I dye (DyNAmo master solution, Finnzymes) and primer set. The PCR conditions were 95°C/10s, 58°C/20s and 72°C/20s, except for rat *Nox1* and rat *Nox4*, in which the annealing temperature was 60°C. The amount of specific mRNA was quantified by determining the point at which the fluorescence accumulation entered the exponential phase (C_t), and the C_t ratio of the target gene to *glyceraldehyde-3-phosphate dehydrogenase* (*Gapdh*) was calculated for each sample. At least two separate experiments were performed for each sample. In some experiments, malignant regions were microdissected from PhIP-induced colon tumors using a Zeiss PALM MicroBeam IV Laser Capture System (Carl Zeiss, Thornwood, NY), and compared with microdissected normal colon. Briefly, mRNA from captured cells was extracted using an RNeasy Micro Kit (Qiagen) and cDNA was synthesized using the Superscript III kit (Invitrogen). Forty-five cycles of qPCR (95°C/10s, 60°C/10s, 72°C/10s) were run on a Roche Light-Cyler 480 II (Roche, Indianapolis, IN), in a 10 μl reaction containing primer set, cDNA and SYBR Green I dye (Roche).

Immunoblotting

ProteoExtract Native membrane protein extraction kit (EMD Biosciences, San Diego, CA) was used for enrichment of membrane proteins, whereas NE-PER reagents (Pierce Biotechnology, Rockford, IL) were used to separate cytoplasmic and nuclear fractions. Membrane-enriched fractions were subjected to SDS-PAGE and immunoblotted using anti-Nox1 (H-75, sc-25545, 1:400 dilution, Santa Cruz Biotechnology, Santa Cruz, CA) and anti-Nox4 (rat, 1:100 dilution, abcam, Cambridge, MA, ab41886; human, 1:500 dilution, Novus, Biologicals, NB110-58851, Littleton, CA). The correct molecular weights were confirmed by reference to the marker

ladder on each blot (Nox1 65-kD, Nox4 67-kD), and antibody specificity was corroborated *via* the use of blocking peptides (sc-5821p against sc-5821 Nox1) (Santa Cruz), 1:200 dilution; Nox4 peptide (ND110-58851 PEP Novus Biologicals), 1:250 dilution). Whole cell lysates were immunoblotted with rabbit polyclonal antibody to IKKα and IKKβ (1:1000 dilution, Cell Signaling, Nos. 2682 and 2684) or phospho-IKKα/β (1:500 dilution, Cell Signaling, no. 2681). Cytoplasmic extracts were probed with antibodies to cleaved caspase 3 (1:1000 dilution, Cell Signaling, no. 9661), cleaved caspase 6 (1:1000 dilution, Cell Signaling, no. 9761), and cleaved caspase 7 (1:1000 dilution, Cell Signaling, no. 9492). Nuclear fractions were immunoblotted with polyclonal rabbit antibody to NFκB p50 (1:600 dilution, Santa Cruz, sc-7178), NFκB p65 (1:600 dilution, Santa Cruz, sc-109), and poly-(ADP-ribose)polymerase (PARP, 1:1000 dilution, Cell Signaling, no. 9532). Amido black staining was used to ensure equal protein loading, followed by β-actin. For nuclear extracts, histone H1 also was used as a loading control (mouse monoclonal antibody sc-8030, Santa Cruz, 1:500 dilution). Proteins were visualized by Western Lightning Chemiluminescence Reagent Plus (Perkin–Elmer Life Sciences, Boston MA), with quantification *via* an AlphaInnotech photodocumentation system and associated software (AlphaInnotech, San Leandro, CA).

Immunohistochemistry

Rat colon tumors were processed to paraffin, sectioned at 4 μm, and placed on charged slides. Sections were rehydrated through xylene, 100% ethanol, 95% ethanol, 80% ethanol and water. Antigen retrieval was carried out in a microwave pressure cooker for 10 min, followed by 20 min at room temperature. Antigen retrieval solution was Dako Target Retrieval Solution pH 6.0 (Dako, Carpentaria, CA). Slides were washed in water and loaded into a Dako autoimmunostainer. Endogenous peroxides were blocked with 3% H_2O_2 in TBST (Dako Tris-buffered saline with Tween 20) for 10 min, and slides were then washed in TBST. Dako serum-free protein block was applied for 10 min, followed by a burst of air to blot the slides. Incubation with the primary antibody was for 30 min (Nox4, 1:250 dilution, Novus Biologicals, NB110-58851, Littleton, CA). As immunohistochemical controls, the corresponding blocking peptide (see above) was used to confirm antibody specificity, and Dako Universal Negative Rabbit control was used in place of the primary antibody. After washing in TBST, Dako Envision+ anti-rabbit HRP was applied for 30 min, followed by Nova Red (Vector Laboratories, Burlingame, CA) and hematoxylin (Dako) counter staining.

The same protocol was used to immunostain Nox4 in human tissues. Tissue microarrays (TMAs) were constructed using a Beecher Instruments MTA-1 tissue arrayer (Beecher Instruments, Sun Prairie, WI). At least duplicate tumor samples were taken from donor tissue blocks, and a retrospective analysis for outcome assessment was based on detailed clinicopathological information linked to the TMA specimens. For further details, see Ashktorab *et al.*[22]

Cell culture, siRNA transfection and LPS treatment

Human colorectal cancer lines HT29 and Caco2 (American Type Culture Collection, Manassas, VA) were maintained in McCoy's 5A medium (Invitrogen) supplemented with 10% heat-inactivated fetal bovine serum (FBS, Hyclone Laboratories), 100 units/ml penicillin, and 100 μg/ml streptomycin at 37°C in 5% CO_2. SmartPool siRNA against human *NOX1* and non-specific control siRNAs were purchased from Dharmacon and transfected according to the manufacturer's instructions. Briefly, cells (1×10^5) were seeded in 6-well plates overnight. The media was aspirated and replaced with fresh antibiotic free-transfection media containing DharmaFECT (4 μl for Caco2 cells, 8 μl for HT29 cells), 100 nM *NOX1* siRNA, or 100 nM non-specific siRNAs (non-target controls), or DharmaFECT only (mock controls). Untreated controls received antibiotic-free media only. At 48 and 72 h after transfection, cells were harvested for flow cytometry, morphological assessment of apoptosis using Acridine Orange/Ethidium Bromide staining, and protein and mRNA analyses. In additional experiments, 72 h after transfection of *NOX1* siRNAs the media was aspirated and replaced with fresh media containing 1.2 μg/μl of LPS (Sigma), or media alone. Thirty minutes later the cells were washed twice with PBS and lysed in IP buffer supplemented with protease inhibitor cocktail and phosphatase inhibitor cocktail I and II (Sigma). Insoluble debris was removed by centrifugation at 10,000g for 5 min at 4°C. Cell lysates were subjected to SDS-PAGE, as described above, and immunoblotted for phospho-IKKα/β (p-IKK, Ser176/180, 1:500, Cell Signaling, no. 2697).

MTT assay

Cells (5×10^3) in 100 μl media were seeded in 96-well plates overnight and transfected with siRNA, as described above. At 24, 48, 72 and 96 h after transfection 3-(4,5-dimethythiazol-2-yl)-2,5-diphenyltetrazolium bromide (MTT) was added and incubated for 3 h, followed by 100 μl of 10% SDS in 0.01 N HCl. Formation of colored formazan dye was assessed colorimetrically at 550 nm.

Cell cycle distribution

Cells treated with *NOX1* siRNA for 72 h (see above) were harvested in cold PBS, fixed in 70% ethanol, and stored at −20°C for 48 h. Fixed cells were washed with PBS and resuspended in propidium iodide/Triton X-100 staining solution containing RNase A. Samples were incubated in the dark for 30 min before determining the DNA content on an EPICS XL Beckman Coulter flow cytometer. Cell cycle distribution was assessed using Multicycle Software (Phoenix Flow Systems, San Diego, CA).

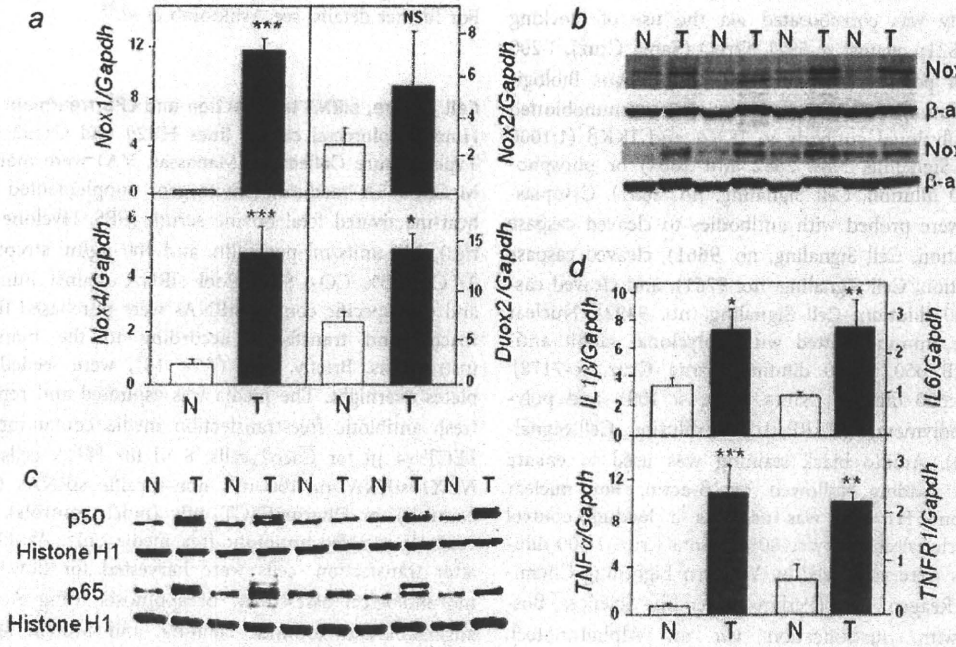

Figure 1. Overexpression of Nox isoforms and NFκB in PhIP-induced rat colon tumors. (*a*) *Nox1*, *Nox2*, *Nox4* and *Duox2* mRNA levels determined by qPCR and normalized to *Gapdh*; solid bars, tumors (T); open bars, adjacent normal-looking tissue (N). (*b*) Immunoblotting of Nox1 and Nox4 proteins in membrane-enriched fractions isolated from rat colon tumors and adjacent normal-looking tissue; loading control, β-actin. (*c*) Immunoblotting of NFκB-p50 and NFκB-p65 proteins in nuclear extracts obtained from rat colon tumors and adjacent normal-looking tissue; loading control, histone H1. (*d*) Expression of NFκB targets *IL1β*, *IL6*, *TNFα* and *TNFR1* in colon tumors and matched normal-looking tissues determined by qPCR. Data = mean ± SE, $n = 9$–12; *$p < 0.05$, **p, 0.01, ***$p < 0.001$.

Cell morphology

Cell suspensions (25 μl) were incubated with 1 μl acridine orange/ethidium bromide solution (50 μg/ml of each reagent in PBS), mixed gently, and placed onto a microscope slide. Cell morphology was examined under a fluorescence microscope for signs of chromatin condensation, fragmented nuclei and/or membrane blebbing, indicative of apoptosis. At least 500 cells were counted per treatment, and three independent experiments were performed.

DNA binding activity of NFκB-p50

Nuclear extracts were examined *via* enzyme-linked immunosorbent assay (NFκB-p50 transcription factor assay kit, Cat no. 10006912, Cayman Chemical, Michigan), according to the manufacturer's instructions.

Statistics

Unless stated otherwise, results shown in each figure were from a single experiment, and are representative of the findings from three or more independent experiments. Data were expressed as mean ± standard error (mean ± SE), and comparisons between control and treatment groups were made using the paired *t*-test (SigmaPlot 8.0). In the figures, significant results were indicated as follows: *$p < 0.05$, **$p < 0.01$ and ***$p < 0.001$.

Results

Nox is overexpressed in PhIP-induced colon tumors

In the colon tumors obtained from rats after 1 year, Nox/Duox mRNA levels were highly overexpressed compared with adjacent normal looking tissue (T *vs.* N in Fig. 1*a*, solid *vs.* open bars). The increase was highly significant for *Nox1* (133-fold, $p < 0.001$) and *Nox4* (6.5-fold, $p < 0.001$), and significant for *Duox2* (2.1-fold, $p < 0.05$), but not significant for *Nox2* (2.0-fold, $p > 0.05$, NS). Adenocarcinoma cells also were captured by laser microdissection from PhIP-induced colon tumors, and these areas expressed significantly increased levels of *Nox1* mRNA (Supporting Information Fig. 2). Because *Nox1* and *Nox4* were most highly overexpressed at the mRNA level, the corresponding proteins were examined by immunoblotting (Fig. 1*b*). After normalizing to β-actin, densitometric analyses confirmed that Nox1 and Nox4 proteins were elevated 2- to 3-fold in tumors *versus* adjacent normal-looking tissue ($p < 0.01$, $n = 12$). A doublet was detected for Nox1, with the upper band stronger in some tumors and the lower band dominating in others (Fig. 1*b*, upper panel). This Nox1 doublet has been observed previously, for example in immortalized human keratinocytes,[23] Ras(+) NIH3T3 cells,[24] rat smooth muscle cells,[25] and human T84 large intestinal cells,[26] but the significance remains unclear. Subsequent studies examined nuclear NFκB

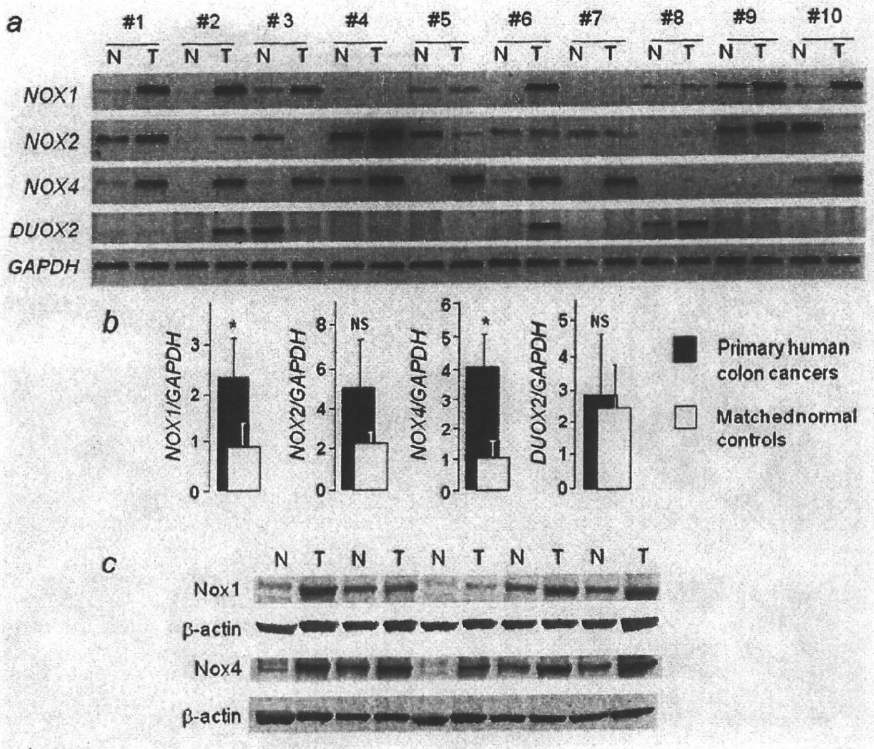

Figure 2. Overexpression of Nox isoforms in human primary colon cancers. (*a*) conventional RT-PCR data for 10 human colon adenocarcinomas (T, tumor) and their matched controls (N, normal-looking tissue from the same patient). (*b*) *NOX/DUOX* mRNA expression in human primary colon tumors determined by qPCR. Data = mean ± SE, $n = 10$; *$p < 0.05$; NS, not significant. (*c*) Immunoblotting of Nox1 and Nox4 proteins in human primary colon tumors and their matched controls.

levels (Fig. 1*c*); after normalizing to histone H1, the increase in both NFκB-p50 and NFκB-p65 protein expression was highly significant in tumors compared with adjacent normal-looking tissue ($p < 0.001$, $n = 12$). qPCR analyses revealed downstream NFκB targets to be increased in colon tumors (Fig. 1*d*), including *IL1β* (2.2-fold, $p < 0.05$), *IL6* (2.9-fold, $p < 0.01$), *TNFα* (16.6-fold, $p < 0.001$) and *TNFR1* (4.0-fold, $p < 0.01$).

Nox is overexpressed in primary human colon cancers

We next examined the expression of Nox/Duox family members in a panel of primary human colon cancers. By conventional RT-PCR (Fig. 2*a*), cancer specimens nos. 1, 2, 3, 6 and 10 had high levels of both *NOX1* and *NOX4* mRNA, whereas *NOX2* and *DUOX2* mRNA levels were more inconsistent, being higher in some cancers and lower or undetectable in others. These findings were confirmed by qPCR, which revealed a 2.5- to 3.0-fold increase in *NOX1* and *NOX4* mRNA expression in primary colon cancers *versus* matched controls ($p < 0.05$, Fig. 2*b*). No significant difference was seen for *NOX2* and *DUOX2* in the qPCR analyses. Thus, Nox1 and Nox4 were selected for subsequent immunoblotting studies (Fig. 2*c*). After normalizing to β-actin, the relative expression in cancers *versus* matched controls was as follows (mean ± SE, $n = 10$): Nox1, 2.36 ± 0.40 *versus* 1.08 ± 0.09 ($p < 0.01$); Nox4, 2.87 ± 0.22 *versus* 1.03 ± 0.09 ($p < 0.001$).

In immunohistochemistry studies, focal areas of intense Nox4 staining were detected in PhIP-induced colon tumors (Fig. 3*a*, right), whereas normal-looking tissue adjacent to the tumor had no such focal Nox4 expression (Fig. 3*a*, left). Staining of serial sections in the absence (Fig. 3*b*) and presence of a Nox4 blocking peptide (Fig. 3*c*) confirmed the specificity of the primary antibody. Cells containing high levels of Nox4 protein typically were interspersed with other cells having little or no such staining. In some of the rat colon tumors, however, islands of intense Nox4 staining were observed, surrounded by areas that were predominantly negative (Fig. 3*d*). These "islands" corresponded to the more differentiated regions within a tumor. In human colon cancer tissue microarrays, a core occasionally stained entirely negative for Nox4 (not shown), but most cores had areas that were strongly Nox4 positive (Fig. 3*e*). Nox4 was detected in the cancer epithelial cells, and was absent from the surrounding stroma (Fig. 3*f*). In some cores, islands of Nox4 staining were associated with differentiated regions within the human

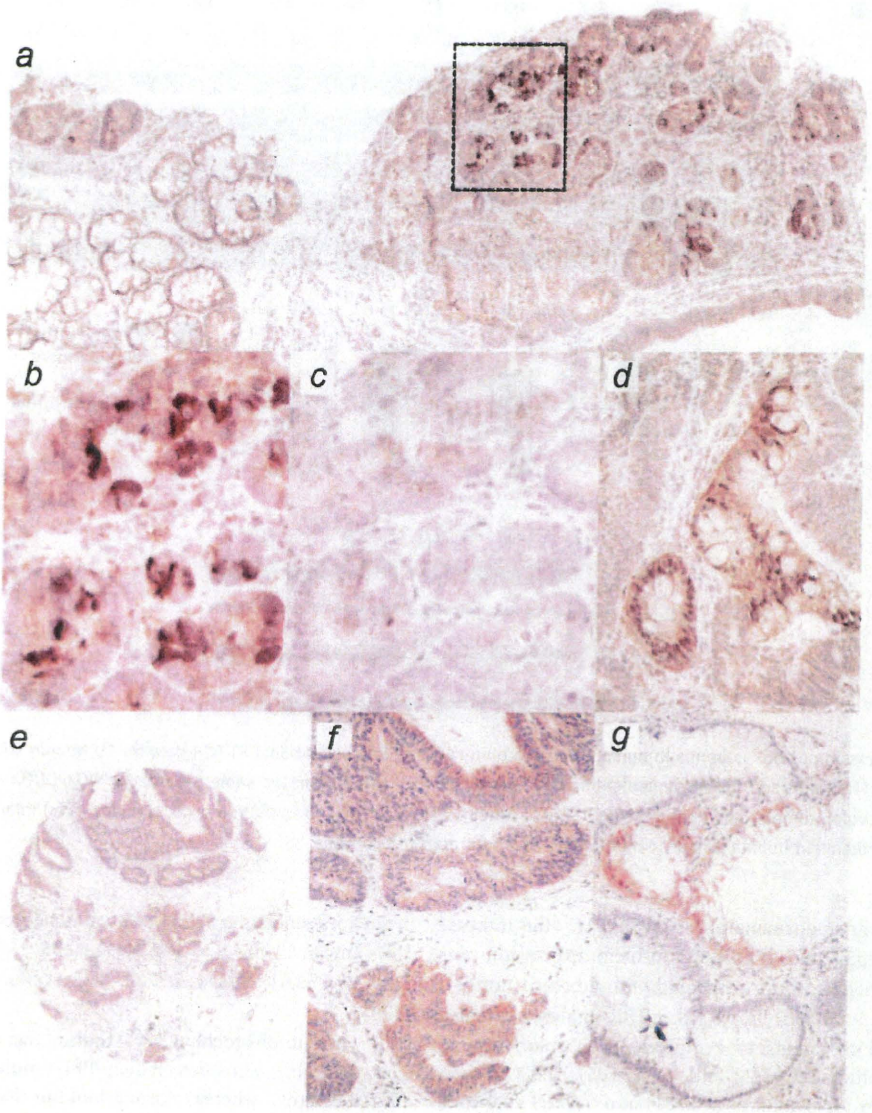

Figure 3. Immunodetection of Nox4 in rat (*a*)–(*d*) and human (*e*)–(*g*) colon tumors. (*a*) Expression of Nox4 in a PhIP-induced colon tumor (right) compared with adjacent normal-looking tissue (left). (*b,c*) Enlarged view of the dotted region from (*a*) showing serial sections stained with Nox4 primary antibody in the (*b*) absence and (*c*) presence of a Nox4 blocking peptide. (*d*) Differentiated regions in a rat colon tumor staining positive for Nox4. (*e*) View of an entire core from a human colon cancer tissue microarray (TMA) immunostained for Nox4, and (*f*) the same core at higher magnification. (*g*) Differentiated regions in a TMA core staining positive for Nox4. [Color figure can be viewed in the online issue, which is available at wileyonlinelibrary.com.]

colon cancer (Fig. 3*g*), as seen in the rat (Fig. 3*d*). Our interpretation is that Nox4 staining patterns were similar in rat and human colon tumors, and that the PhIP model might provide useful insights into the role of Nox4 in colon cancer development.

Attempts to immunolocalize Nox1 protein in rat and human colon tissues were unsuccessful. In our hands, antibodies from commercial sources (cs-25545 from Santa Cruz, ab78016 from abcam, and LS-B1832 from Lifespan Biosciences, Seattle, WA) gave high background expression with nonspecific labeling, despite exhaustive protocol modifications and antibody dilution experiments (data not shown).

Nox1 knockdown induces cell cycle arrest and apoptosis

HT29 and Caco2 cells were selected from among a panel of human colon cancer cell lines due to their high *NOX1* mRNA content (data not shown), and *NOX1* siRNA was used as a knockdown strategy. Based on the results of three

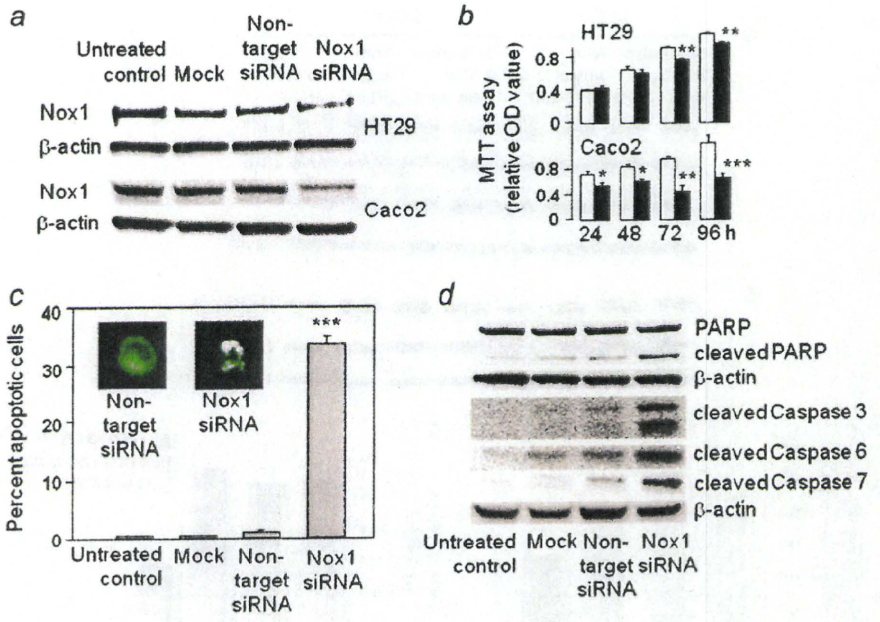

Figure 4. Nox1 knockdown in human colon cancer cells. (*a*) Immunoblot analyses of Nox1 expression in HT29 and Caco2 cells treated with *NOX1* siRNA or nontarget siRNA. Untreated and mock controls (transfection agent alone) were included in the assays. (*b*) MTT assay data following *NOX1* siRNA (solid bars) or nontarget siRNA (open bars); mean ± SE, $*p < 0.05$, $**p < 0.01$, $***p < 0.001$, $n = 3$. (*c*) Percent apoptosis in Caco2 cells, 72 h after treatment with Nox1 siRNA (mean ± SE, $n = 3$; $***p < 0.001$ *versus* nontarget siRNA); inset: acridine orange/ethidium bromide dual staining showing nuclear condensation and other hallmarks of apoptotic morphology. (*d*) Cleavage of PARP and caspases 3, 6, and 7, 72 h after *NOX1* knockdown in Caco2 cells. Caspase-3 cleaved products, 17-kD and 19-kD. [Color figure can be viewed in the online issue, which is available at wileyonlinelibrary.com.]

replicate qPCR experiments, *NOX1* mRNA levels in HT29 cells typically were diminished by 48% at 48 h and 92% at 72 h, whereas in CaCo2 cells the reduction was 60% at 48 h and 94% at 72 h. Despite the similar knockdown efficiency for *NOX1* mRNA at 72 h, Nox1 protein expression was reduced more dramatically in Caco2 cells than in HT29 cells (Fig. 4*a*). Densitometry measurements were performed on Nox1 normalized to β-actin. Compared with the non-target siRNA control at 72 h, the relative expression of Nox1 protein was reduced by 48% in HT29 cells (1.03 ± 0.12 *vs.* 0.54 ± 0.07, $p < 0.05$) and by 82% in Caco2 cells (0.96 ± 0.07 *vs.* 0.18 ± 0.05, $p < 0.001$).

Inhibitory responses in the MTT assay following Nox1 knockdown were significant at all time-points after 24 h in Caco2 cells, and after 72-96 h in HT29 cells (Fig. 4*b*). To clarify whether the MTT assay data might be indicative of changes in cell cycle kinetics or apoptosis, further experiments were performed. In HT29 cells, changes in the cell cycle were detected 72 h post-transfection, as follows: 77.4 ± 2.5% *versus* 52.5 ± 2.9% in G1, 14.6 ± 2.2% *versus* 30.5 ± 1.6% in S, and 8% *versus* 16.6% in G2/M (*NOX1* siRNA *vs.* nontarget siRNA, mean ± SE, $n = 3$ separate experiments). No significant changes were detected in the proportion of HT29 cells undergoing apoptosis (2–3% in all groups, data not shown). In contrast, Caco2 cells exhibited clear hallmarks of apoptosis (Fig. 4*c*, inset), and the percentage of apoptotic cells at 72 h increased from 1-2% after exposure to non-target siRNA to >30% following treatment with *NOX1* siRNA ($p < 0.001$). In Caco2 cells treated with *NOX1* siRNA, there was an increase in the cleaved (active) forms of Caspase-3, -6 and -7, as well as elevated PARP cleavage (Fig. 4*d*). Taken together, these findings suggested that human colon cancer cells undergo cell cycle arrest or apoptosis, depending on the cell line and extent of Nox1 knockdown.

Nox1 knockdown blocks LPS-induced IKK phosphorylation and NFκB activity

In HT29 cells, low constitutive levels of phospho-IKK were detected in the absence of LPS treatment, whereas an increase in phospho-IKK was evident within 30 min of LPS exposure (Fig. 5*a*, LPS− *vs.* LPS+, respectively). Interestingly, LPS-induced phospho-IKK expression was blocked in cells that had been transfected with *NOX1* siRNA (Fig. 5*a*, top right). When the nuclear extracts were examined 6 h after treatment with LPS or media alone, NFkB-p50 and -p65 proteins were reduced markedly by Nox1 knockdown (Fig. 5*b*). Knockdown of Nox1 reduced significantly the DNA binding activity of NFκB in nuclear extracts ($p < 0.05$, Fig. 5*c*), and lowered the mRNA expression levels of downstream NFκB targets, such as *MYC*, *CCND1* and *IL1β* ($p < 0.05$, Fig. 5*d*).

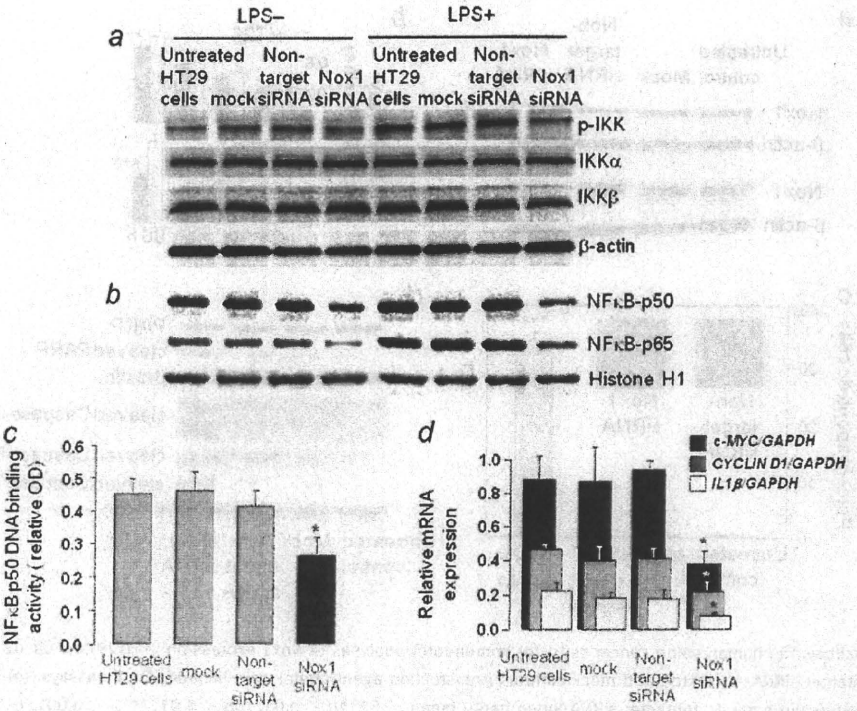

Figure 5. Nuclear NFκB expression and DNA binding activity following Nox1 knockdown in human colon cancer cells. (*a*) Seventy-two hours after transfection with *NOX1* siRNA, HT29 cells were treated with LPS (1.2 μg/ml) or media alone for 30 min, and whole cell lysates were immunoblotted for phospho-IKKα/β (p-IKK), IKKα, or IKKβ, with β-actin as loading control. (*b*) Nuclear extracts were immunoblotted for NFκB-p50 and NFκB-p65, 72 h after HT29 cells were treated with *NOX1* siRNA, and 6 h following treatment with LPS or media alone. (*c*) NFκB (p50) DNA binding activity in nuclear extracts from HT29 cells, 72 h after Nox1 knockdown. Data = mean ± SE, $n = 3$; $^*p < 0.05$ *versus* the corresponding nontarget siRNA control. (*d*) c-*MYC*, *CYCLIN D1* and *IL1β* mRNA expression following Nox1 knockdown; qPCR data normalized to *GAPDH*; mean ± SE, $n = 3$; $^*p < 0.05$ *versus* the corresponding nontarget siRNA control.

Discussion

Oxidative stress in the colon originally was thought to involve Nox2, and was ascribed to resident and recruited phagocytic cells with important roles in host-defense mechanisms.[7,27] However, this idea has evolved with the discovery of non-phagocyte derived Nox/Duox homologues. Nox1 is expressed in gastric pits and colonic epithelial cells and is required for normal gut physiology. For example, Nox1-induced oxidative stress, involving intermediates such as $O_2^{\bullet-}$ and H_2O_2, regulates mucosal 5-hydroxytryptamine levels, which affects normal secretion and motility in the colon.[28] Transcriptional activation of *NOX1* by IFN-γ produces $O_2^{\bullet-}$ in colonic epithelial cells, contributing to mucosal host defense mechanisms.[26] Duox2 is expressed in normal human colorectal barrier epithelial cells,[16] and its loss following *duox2* silencing in flies markedly enhances mortality following infection.[29] Nox family members also have been implicated in Crohn's disease and other inflammatory bowel disorders.[7]

Although the cancer-associated expression of Nox1 has been reported in human stomach,[30] there is some debate over the precise role of Nox1 in colon cancer, as noted in the introduction. The most recent study found that Nox1 was overexpressed in human colon cancers and was correlated with activating mutations in K-ras.[19] Colon tumors induced by PhIP and other heterocyclic amines lack mutations in K-ras, but harbor genetic changes in β-catenin or Apc.[20,21,31] We performed mutation screening for the corresponding genes in the PhIP-induced colon tumors reported here, but observed no correlations with the expression of Nox1 or other Nox/Duox members (data not presented). Nonetheless, results from the present investigation support a role of Nox1 in human colon cancer and expand this observation to Nox4, including the first such evidence using a rat colon carcinogenesis model.

Interestingly, increased Nox1, NFκB-p50, and NFκB-p65 protein levels were detected in colonic mucosa obtained from rats immediately after completing PhIP treatment, several weeks before the appearance of frank tumors (Supporting Information Fig. 3). Thus, Nox1, NFκB-p50, and NFκB-p65 might play a role during the early stages of PhIP-induced colon carcinogenesis. Charalambous *et al.*[32] recently postulated